Adiabatic Passage by Light-Induced Potentials in Polyatomic Molecules†

Jesús González-Vázquez, Ignacio R. Sola,* and Jesús Santamaría

Departamento de Química Física, Universidad Complutense, 28040 Madrid, Spain

Received: July 15, 2005; In Final Form: August 30, 2005

In this paper we study the first application of adiabatic passage by light-induced potentials in polyatomic molecules. We analyze the effects of increasing the dimensionality of the system on the adiabatic requirements of the method and the role of intramolecular coupling among the vibrational modes. By using a model of two-dimensional displaced harmonic oscillators with or without rotation of the normal mode axis of the excited states (Duschinsky effect) we find that (1) it is possible to selectively transfer the vibrational population by adiabatic elongation of the bonds, (2) the adiabatic demands depend mainly on the energy barrier between the ground and excited electronic configurations, and not on the dimension of the system, (3) in the presence of intramolecular couplings the selective transfer can be achieved but at the cost of increasing the duration and/or the intensity of the pulses, which are needed to overcome small avoided crossings, and (4) the problem of selectivity becomes more important as the vibrational energy of the initial wave function increases.

1. Introduction

The selective preparation of molecules in specific quantum states is still one of the paradigm examples of Quantum Control, with potential applications in molecular spectroscopy and chemical reactivity.[1−3] Among the many techniques of quantum control, there has been a growing interest in developing adiabatic passage methods.[4,5] The adiabatic passage dynamics does not depend on detailed quantum phase interference processes and is usually more robust to the different pulse parameters and fluctuations.[4,5] Additionally, it allows a systematic study of the scaling properties and the different physical resources that are needed for the schemes to adequately operate.

In this work we apply a well-known scheme where the adiabatic passage is controlled by counterintuitive pulse sequences. Using moderately intense and long pulses, the scheme, known as StiRAP[6−8] (Stimulated Raman Adiabatic Passage), implies a fine-tuning of the Hamiltonian to allow resonant two-photon state-to-state adiabatic passage between the initial and target vibrational wave functions, bypassing an intermediate, not populated state, that works as a "wave function bridge" connecting both states.[9]

Using stronger and shorter pulses, Garraway and Suominen proposed the APLIP (adiabatic passage by light-induced potential) scheme.[10] The strong pulses modify the structure of the electronic potential, mixing different electronic states, which thus exhibit "intermediate" properties.[11,12] In APLIP, this adiabatic potential modulated by the laser pulses (or LIP[13]) correlates at the initial time with the ground electronic state and at the final time with the desired excited potential. At all times the LIP has a well defined structure, with laser-controlled, smoothly changing properties, so that the wave function can adiabatically move from the initial state to the desired target wave function. The spatial adiabaticity of the wave packet motion ensures that the nodal pattern of the wave function is conserved during the transfer. Therefore, the selective wave function transfer implies a mapping of the original wave function onto the excited potential. This mapping is unique for diatomic molecules (one-dimensional wave functions), but this is not necessarily the case for N-dimensional systems. In passing, we note that there are other schemes that allow fast adiabatic passage via dissociative states, as in the time-gating scheme,[14] although probably with less final selectivity, since the wave function is not an eigenstate of the LIP.

Until now, several extensions of the APLIP scheme have been proposed,[15−19] although no experimental results are still available. All the work has been related to simple diatomic molecules. In this paper we propose and test the first application of APLIP to polyatomic molecules. We use a two-dimensional dynamical model (two vibrational modes) with harmonic potentials to address mainly two questions: (1) can a multidimensional wave packet be transferred by the APLIP scheme and how does the physical resources scale with the dimensionality and (2) how is the adiabatic motion of the wave packet affected by intramolecular couplings, or alternatively, how can the original wave function be mapped on the excited potential when the assignment of vibrational quanta differs in both potentials.

To explain in more detail the dynamical mechanism of APLIP, we shall use now an example of dynamics in a two-dimensional potential. As in most molecules, the equilibrium configuration of the target electronic state is displaced to a larger bond distance in both vibrational modes, while we need as well an intermediate electronic potential which we also consider with a displaced equilibrium configuration (although the intermediate potential features practically do not affect the dynamics of the system). In APLIP, the one-photon transition between the ground and intermediate excited state is broadly shifted to the blue of the resonance[20] so that the intermediate potential is barely populated. In Figure 1 we show the results of the dynamics when we apply a counterintuitive sequence of strong nonresonant pulses. The result is obtained solving the Schrödinger equation of the system, and details about the model and the numerical procedure are given in the next section.

The dynamics can be explained in terms of a simple electronic lever mechanism induced by a clever choice of timing and

† Part of the special issue "William Hase Festschrift".

* To whom correspondence should be addressed. E-mail: ignacio@tchiko.quim.ucm.es.

10.1021/jp0539021 CCC: $33.50
Published on Web 10/12/2005

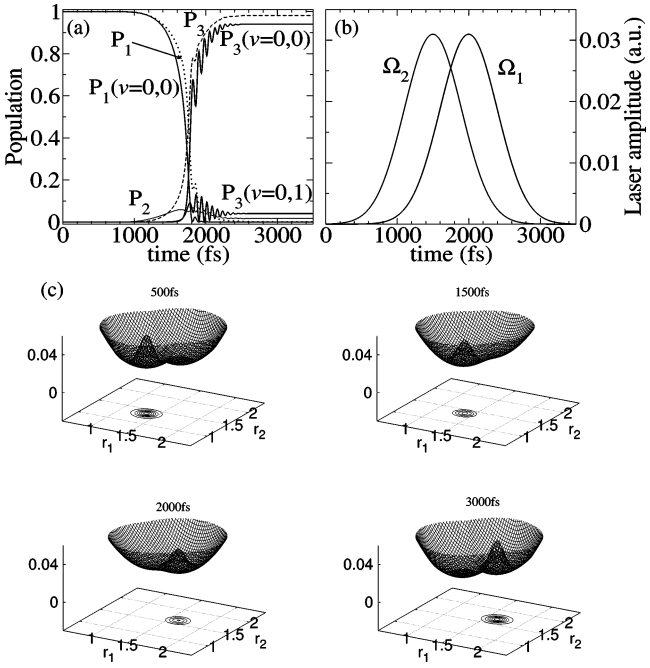

Figure 1. Dynamics of APLIP to an excited potential with displaced equilibrium configuration in two normal modes. In (a) we show the population dynamics, in (b) the pulse profiles, and in (c) snapshots of the wave packet in the light-induced potential at different times, exhibiting the sequential steps of the APLIP mechanism.

direction of the induced Stark-shifts.[10,15,9] To understand it, it is convenient to dress the potentials with the photon energies. In APLIP, $V_1(r_1, r_2) + \hbar(\omega_1 + \omega_2)$ is in resonance with $V_3(r_1, r_2)$ but blue-shifted from $V_2(r_1, r_2) + \hbar\omega_2$. In the adiabatic representation (see Figure 1) the initial LIP is a double well potential, with the closer (left) well representing the ground equilibrium configuration, and the further (right) well representing the excited equilibrium configuration. Notice that the desired two-photon transition from the ground eigenstate of V_1 to the ground eigenstate in V_3 is a highly non-Franck−Condon transition that must drive the wave packet from the bottom of one well to another. This can be done in a tunneling fashion,[12] involving only the initial and final levels (as it occurs in StiRAP) or by promoting the wave packet over the energy barrier, as in APLIP.

The APLIP mechanism works in the following way. First the second pulse, coupling V_2 with V_3 is switched on. The strong nonresonant field induces a Stark-shift that lifts the right well increasing the energy barrier. However, as the second pulse decreases and the first pulse (coupling V_1 with V_2) increases, the left well is lifted over the right well, allowing the wave packet transfer. In fact, in the adiabatic representation the energy barrier is suppressed by the strong fields, so that the LIP has a single well. Thus, the wave packet is trapped at the bottom of the potential during all the transfer and the dynamics is "spatially" adiabatic. Finally, both pulses are switched off, and the shape of the initial LIP is restored with the wave packet at the bottom of the right well.

As Figure 1 shows, in the energy representation the motion of the wave packet from one configuration to the other involves the transient excitation of several excited vibrational eigenstates, first of V_1 and then of V_3, so that in the diabatic representation the average energy of the wave packet at intermediate times is above the energy barrier. This is in stark contrast to the StiRAP process, where only the initial and target states are populated, as the dynamics proceeds in a tunneling fashion.[12]

TABLE 1: Hamiltonian Parameters for the Symmetric (SPM) and Asymmetric (APM) Potential Models

	SPM		AMP	
	r_1	r_2	r_1	r_2
G_{ii}^{-1} (au)	21600	43200	21600	21600
F_{ii} (au)	0.4	0.4	0.2	0.1
ω (cm^{-1})	609	430	609	430

The remainder of the paper is organized as follows. In section 2 we detail the Hamiltonian of the system. We use simplified models with the goal of analyzing the essential features of polyatomic molecular dynamics that can affect the outcome of the APLIP process. The results of the APLIP process are given in sections 3−5. In section 3 we consider the APLIP dynamics and the onset of adiabatic conditions when the excited-state equilibrium configuration is displaced in one or more normal modes, that is, when the transfer process implies a translation of the wave function in one or two dimensions. In section 4 we consider the case where the normal mode axis in the target state are rotated with respect to those of the ground state. This physical process is called the Duschinsky effect[21,22] inducing the coupling between the vibrational modes in the Hamiltonian, analogous to what occurs in other intramolecular processes. In this case, the APLIP transfer implies the rotation of the wave function. In section 5 we consider the case of translation and rotation of the wave function. Finally, section 6 is the conclusions.

2. Molecular Model with Two Vibrational Coordinates

To address the viability of APLIP in polyatomic molecules, we consider a simple molecular model of three electronic potential surfaces with two active vibrational modes coupled by two laser pulses. We assume the rotating wave approximation[23] and two-photon resonance between the initial and second excited electronic potential, with general Hamiltonian

$$\mathscr{H} = \begin{pmatrix} \mathbf{T}_1 & 0 & 0 \\ 0 & \mathbf{T}_2 & 0 \\ 0 & 0 & \mathbf{T}_3 \end{pmatrix} + \begin{pmatrix} V_1(r_1,r_2) & -\Omega_1(t)/2 & 0 \\ -\Omega_1(t)/2 & V_1(r_1,r_2) - \Delta & -\Omega_2(t)/2 \\ 0 & -\Omega_2(t)/2 & V_3(r_1,r_2) \end{pmatrix} \quad (1)$$

The different terms entering in the Hamiltonian are as follows:

(1) $\mathbf{T}_i = -\hbar^2/2G_{11}^{(i)}\partial^2/\partial r_1^2 - \hbar^2/2G_{22}^{(i)}\partial^2/\partial r_2^2 - \hbar^2 G_{12}^{(i)}\partial^2/\partial r_1 r_2$ is the kinetic energy term associated to the (normal) modes r_1 and r_2. The mass-related coefficients are typically the same for the different electronic states (see Table 1), but we allow for a kinetic energy coupling term in the final potential (changes in the intermediate potential barely affect the APLIP process) which implies a rotation in the normal coordinates of the excited state with respect to the normal coordinates defined for the ground potential (Duschinsky effect). Therefore, we can write $\mathbf{T}_1 = \mathbf{T}_2 = \mathbf{T}$ and $\mathbf{T}_3 = \mathbf{T} + \mathbf{T}_c$, where $\mathbf{T}_c$ is the kinetic coupling term (when $G_{12}^{(3)} \neq 0$). In section 4 we explain how we model the effect of this coupling.

(2) $V_j(r_1, r_2)$ are the potential energy surfaces in the normal vibrational modes r_1 and r_2. We choose harmonic potentials $V_i(r_1, r_j) = 1/2F_{11}^{(i)}(r_1 - r_{1,0}^{(i)})^2 + 1/2F_{22}^{(i)}(r_2 - r_{2,0}^{(i)})^2 + F_{12}^{(i)}(r_1 - r_{1,0}^{(i)})(r_2 - r_{2,0}^{(i)})$. In different simulations we vary the displacement $\vec{d}$ between the potential minima as $\vec{r}_0^{(3)} = \vec{r}_0^{(1)} + \vec{d} = \vec{r}_0^{(2)} + \vec{d}/2$ (where $\vec{r}_0^{(i)} = (r_{1,0}^{(i)}, r_{2,0}^{(i)})$, and the intermediate excited potential is symmetrically displaced). By definition, the rectilinear normal modes are uncoupled in the harmonic approximation ($F_{12}^{(i)} = 0$). However, when the normal coordinates of the

excited potential are rotated, $\vec{r}^{(3)} = \mathbf{R}(\theta)\vec{r}^{(1)}$ ($\mathbf{R}(\theta)$ is a rotation matrix), they induce the coupling between the two oscillators in the normal coordinates defined by the ground state, given by $F_{12}^{(3)}$. In section 4 we explain how we estimate $F_{12}^{(3)}$ in the frame of the Duschinsky effect. The Hamiltonian parameters for the system models are given in Table 1.

(3) $\Delta = 0.02$ au ($\sim$4400 cm^{-1}) is the one photon blue-shifted detuning, which we fix in all simulations.

(4) $\Omega_1(t)$ and $\Omega_2(t)$ are the Rabi frequencies. We choose Gaussian-shaped laser pulses in counterintuitive order, so that for a conveniently chosen initial time we write

$$\Omega_1(t) = \mu_{12}\epsilon_0 \exp\left(\frac{-t}{2\sigma}\right)^2 \tag{2}$$

and

$$\Omega_2(t) = \mu_{23}\epsilon_0 \exp\left(\frac{-(t-\tau)}{2\sigma}\right)^2 \tag{3}$$

Both pulses have the same shape and are just shifted in time, where σ is the time-width of the lasers and τ is the (positive) time delay. We assume the Franck−Condon approximation with a unit dipole moment, $\mu_{ij}(r_1, r_2) = 1$, allowing both modes to be coupled to the radiation. ϵ_0 is the peak amplitude. We consider two different time-durations: For shorter pulses $\sigma =$ 400 fs, $\tau = 500$ fs, while for longer pulses we set $\sigma = 2.4$ ps and $\tau = 3$ ps.

The Schrödinger equation is solved using the Split-Operator method to second-order coupled to Fast-Fourier Transform grid techniques.[24] The potential energy term in the split-propagator is diagonalized at each instant of time. In the presence of kinetic energy intramolecular coupling, a further approximation is introduced by splitting the kinetic energy term using

$$\exp(\alpha H) \approx \exp\left(\frac{\alpha}{2}v\right)\exp\left(\frac{\alpha}{2}\mathbf{T}\mathscr{I}\right)\exp(\alpha\mathbf{T}_c\delta_{13}\mathscr{I})\exp\left(\frac{\alpha}{2}\mathbf{T}\mathscr{I}\right)\exp\left(\frac{\alpha}{2}v\right) \tag{4}$$

where $\alpha = -i\Delta t/\hbar$, v is the potential energy matrix, $\mathscr{I}$ is the unit matrix, and we assume that the coupling only appears in the final excited potential when the normal mode axis are rotated. $\mathbf{T}_c$ involves a two-dimensional Fast Fourier transform. In all simulations we start in an eigenstate of the Hamiltonian, denoted by the normal mode quantum numbers (v_1, v_2) of the ground electronic state.

3. Adiabatic Passage as a Function of the Vibrational Mode Displacement

In this section we compare the APLIP performance when the displacement between the equilibrium position of the $V_1(r_1, r_2)$ and $V_3(r_1, r_2)$ electronic potentials $\vec{d} = (d_1, d_2)$, changes in either one or both coordinates, that is, when the equilibrium configuration of one or both vibrational modes is displaced in the electronic excited states. All results are obtained using the same force (F_{ii}) and kinetic (G_{ii}) matrix elements for all the electronic potentials, following the SPM model parameters shown in Table 1.

Obviously, the APLIP process can occur in both cases, as shown in the Introduction, but the effort or physical resources needed to obtain high yields of population transfer depends on the direction of the displacement. In Figure 2 we show the variation of the yield of APLIP as a function of the pulse peak amplitude (or peak intensity) for two cases, $\vec{d} = (0.3, 0)$ au and $\vec{d} = (0, 0.3)$ au. In the first case a smaller pulse amplitude is needed in order to reach the adiabatic threshold, which we arbitrarily fix when a yield larger than 0.95 is achieved. We can define two different thresholds: the electronic threshold ξ_e, that measures the intensity demands to drive the electronic population to V_3, and the selective threshold ξ_s, which considers selective excitation of a single vibrational target state on V_3. Starting in (v_1, v_2), a selective APLIP process should prepare the system in the same vibrational wave function of the excited potential. This can be explained by the "spatial" adiabaticity of the dynamics: a wave function can be distorted but cannot change the nodal patterns when the dynamics is adiabatic. The spatial adiabaticity is more time and energy demanding than just the electronic excitation, since not only the energy barrier must be removed but also the LIP must have all the time a stable equilibrium configuration where the wave packet is located and must change smoothly from one configuration to another. These requirements imply that the difference between ξ_s and ξ_e usually increases with the wave packet displacement.[9]

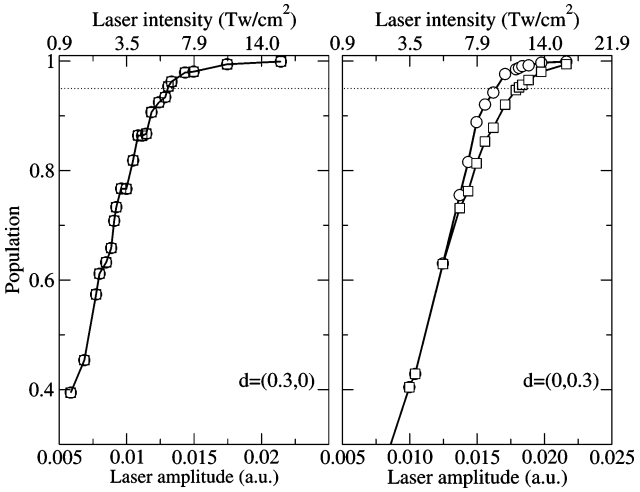

Figure 2. Electronic (P_3) and vibrational population on the target state [$P_3(v = 0)$] in APLIP as a function of the pulse amplitude (lower scale) or intensity (upper scale) for two different excited potentials. We fix the adiabatic threshold when the population is larger than 0.95.

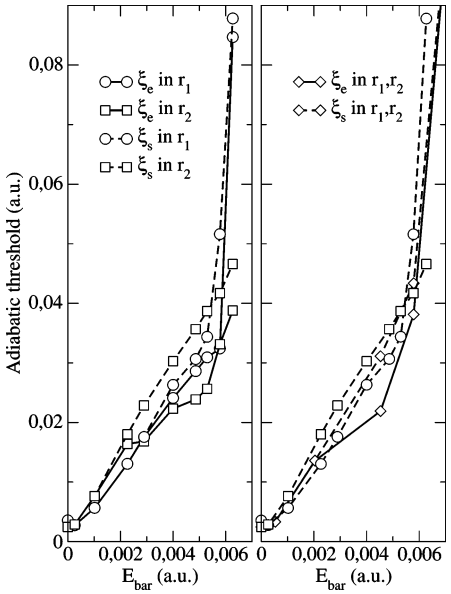

Figure 3. Adiabatic thresholds as a function of the energy barrier, when the excited state is translated in one (r_1 or r_2) or both vibrational modes.

In Figure 3 we show the variation of the APLIP thresholds as the equilibrium distance in V_3 is shifted along r_1 or r_2. Notice that the electronic potential is symmetric in both coordinates,

and therefore the energy barrier E_{bar} does not depend on the direction of displacement. However, since G_{22} is smaller than G_{11} (for equal force constant), $\omega_2 < \omega_1$ and the wave packet needs more energy from the pulse to overcome the barrier. Hence, the adiabatic threshold is shifted to higher pulse intensities when the bond is elongated along r_2. For larger bond displacements (large E_{bar}) the adiabatic thresholds increase considerably. This is partially because as we fix the detuning the required Rabi frequencies become much larger than Δ. Then, more extra energy is needed to avoid the flow of population to V_2 and sustain the adiabatic passage regime.[9]

A good way of considering the intensity demands is in terms of E_{bar} divided by the vibrational quanta, ω_1 and ω_2, which gauges the average vibrational excitation of the wave packet needed to overcome the barrier. For instance, if $\vec{d} = (0.4, 0)$ au, then $E_{bar} = 4 \cdot 10^{-3}$ au, and $E_{bar}/\omega_1 = 1.3$, so that the wave packet must be excited over (1, 0) in the ground potential (and in the excited potential as well). However, for $\vec{d} = (0, 0.4)$ au the same energy barrier implies $E_{bar}/\omega_2 = 1.9$, so that on average, the wave packet must be excited over the vibrational state (0, 2) before reaching the target state.

From a different perspective, the same reasons imply that the initial wave packet is more squeezed in the r_2 mode than in r_1. The overlapping between the initial state and the target state is therefore smaller, and the APLIP dynamics involves considerable transient excitation of other vibrational states both in $V_1(r_1, r_2)$ and $V_3(r_1, r_2)$ as the wave packet moves along r_2. Conversely, the overlapping is larger when the displacement occurs along the r_1 mode, so that in this case almost only the initial and final vibrational states are populated and the two-state dynamics are very similar to that of StiRAP.[6,5] In fact, for $\vec{d} = 0$ the APLIP and StiRAP dynamics converge.[9] This is why the electronic and selective thresholds are approximately the same when the wave packet moves along r_1 but depart when the wave packet moves along r_2 (obviously with $\xi_s > \xi_e$).

The equilibrium position of V_3 can also be displaced along both normal modes. In Figure 1 we showed a typical APLIP dynamics in the adiabatic representation, following the wave packet in the LIP $U_0(r_1, r_2, t)$, for $\vec{d} = (0.3, 0.3)$ ($|\vec{d}| = 0.42$, $E_{bar} = 4.5 \cdot 10^{-3}$). Since the harmonic potentials in the model are symmetric, E_{bar} depends only on the distance $|\vec{d}|$, not the direction. We expect the threshold of adiabatic passage to be approximately between those for displacement along r_1 and r_2 alone, since we can define an "average" vibrational quantum to gauge the magnitude of E_{bar}, which will be between ω_1 and ω_2. This behavior is observed to be approximately correct, as Figure 3 shows.

Additionally, we have tested the dependence of the adiabatic thresholds on the initial state. As noted, the APLIP dynamics maps the initial wave function onto the final potential. Fixing the displacement as $\vec{d} = (0.3, 0.3)$, in Figure 4 we have calculated the electronic and selective thresholds. Both ξ_e and ξ_s increase with the quantum numbers. This effect cannot be explained by the energy barrier, which in fact is smaller for an excited vibrational wave function. We believe that the underlying reason is due to "spatial" adiabaticity requirements. For increasing quantum numbers, the energy separation between adjacent vibrational eigenstates tends to decrease even for harmonic potentials in polyatomic molecules, since the vibrational quanta can be shared between different modes with similar frequencies. Thus the need to increase ξ_s (and ξ_e) in order to satisfy the adiabatic demands. The same rule seems to apply for a given quantum depending on its distribution among the modes. The greater the energy ($\omega_1 > \omega_2$) the greater the adiabatic thresholds. Another possible way to improve the adiabaticity implies using longer pulses. Then ξ_s can remain constant.

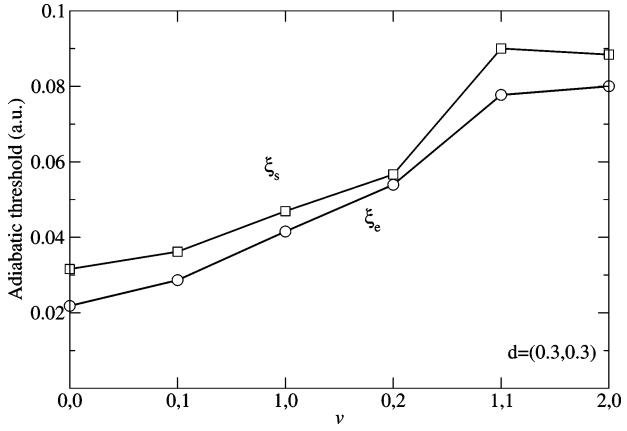

Figure 4. Adiabatic thresholds as a function of the initial state, for an excited potential with equilibrium configuration shifted to $d = (0.3, 0.3)$.

4. Adiabatic Excitation between Electronic Potentials with Rotated Normal Modes

The normal modes are linear combinations of the local modes typically obtained by diagonalizing the Hessian matrix.[25] This linear combination can be different in the excited potential, leading to a rotation of the vibrational wave functions of the excited state related to the normal axis for the ground potential. This is usually called the Duschinsky effect.[21,22] The APLIP method maps the initial wave function onto the final potential conserving the vibrational quanta. We want to test if this mapping is affected (and how) by the rotation of the vibrational mode axis, and thus of the linear combination that defines the vibrational quanta at the target state. In this section we consider the unusual case when the equilibrium configuration of $V_3(r_1, r_2)$ is only rotated with respect to that of $V_1(r_1, r_2)$, while in the next section we consider both rotation and translation of the excited potential.

To model the effect of rotated normal modes, we first consider that the normal modes of V_3 are rotated by $\mathbf{R}(\theta)$ with respect to those in V_1 ($\vec{r}' = \mathbf{R}(\theta)\vec{r}$), and since the dynamics is followed in the grid mapped onto the last ones, we calculate $V_3(\mathbf{R}^{-1}\vec{r})$ and $\mathbf{R}^{-1}\mathbf{T}\mathbf{R}$, obtaining

$$V_3(r_1, r_2) = (F_{11}\cos^2\theta + F_{22}\sin^2\theta)(r_1 - r_{1,0})^2 + (F_{11}\sin^2\theta + F_{22}\cos^2\theta)(r_2 - r_{2,0})^2 + (F_{11} - F_{22})\sin 2\theta(r_1 - r_{1,0})(r_2 - r_{2,0}) \quad (5)$$

and

$$\mathbf{T}_3 = -\frac{\hbar^2}{2}(G_{11}\cos^2\theta + G_{22}\sin^2\theta)\frac{\partial^2}{\partial r_1^2} - \frac{\hbar^2}{2}(G_{11}\sin^2\theta + G_{22}\cos^2\theta)\frac{\partial^2}{\partial r_2^2} - \frac{\hbar^2}{2}(G_{11} - G_{33})\sin 2\theta\frac{\partial}{\partial r_1}\frac{\partial}{\partial r_2} \quad (6)$$

where we have assumed that the force and kinetic matrix elements as well as the equilibrium configuration are the same in both $V_1(\vec{r})$ and $V_3(\vec{r}')$ (thus in eqs 5 and 6 we have dropped all superindexes identifying the electronic state). Notice that the rotation of the normal axis introduces coupling terms between the modes in both kinetic $\mathbf{T}_c$ and potential $V_c(r_1, r_2)$ energies. The rotation of the axis is a convenient way of

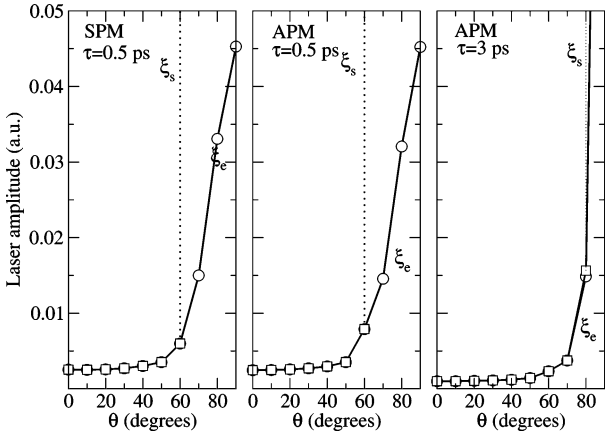

Figure 5. Adiabatic thresholds in APLIP with Duschinsky rotation in the excited potential for the SPM and the APM using shorter and longer pulses. The initial state is (0, 1). ξ_s blows up after a certain angle of rotation.

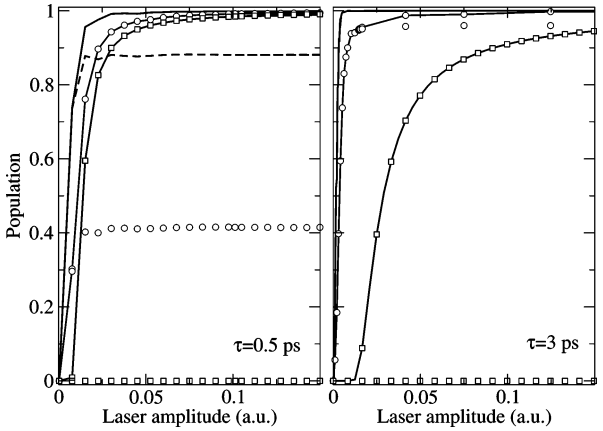

Figure 6. Final population in APLIP with Duschinsky rotation in the excited potential as a function of the laser amplitude using shorter (left) and longer (right) laser pulses. The initial state is (0, 1). Electronic populations are in solid lines for $\theta = 70°$, 80° (line with circles) and 90° (line with squares), while the target population in (0, 1) are in broken line for $\theta = 70°$ or in circles (80°) and squares (90°) without line.

including the coupling between the modes, which allows a systematic comparison of the results as a function of a single parameter, the angle of rotation θ. In general, the terms V_c and $\mathbf{T}_c$ are not necessarily related, since other physical effects may originate the intramolecular coupling between the modes. However, the physical effects that they cause in the dynamics are essentially the same, and therefore we expect our simple models to provide quite general trends regarding the adiabatic dynamics in realistic molecules.

We consider two set of parameters in the Hamiltonian. In the first model, that we call the symmetric potential model (SPM), the Duschinsky effect only induces kinetic couplings. We also consider a second set of parameters with equal mass terms (see Table 1) so that the couplings only enter in the potential energy. This case, the asymmetric potential model (APM), allows a simpler integration of the Schrödinger equation, since $\mathbf{T}_c = 0$ (see section 2).

In Figure 5 we show the electronic and selective adiabatic thresholds as a function of the angle of rotation θ, for both SPM and APM and different pulse durations, starting from two different vibrational eigenstates, (0, 0) and (0, 1). Since V_3 is only rotated with respect to V_1, there is no E_{bar} for the adiabatic transfer. However, the transfer depends on the angle of rotation. First, due to the symmetry of the Hamiltonian, the results are the same for $\pi/2 \pm \theta$, so that we only show ξ_e and ξ_s up to 90°.

Since (0, 0) is almost spherically symmetric, the thresholds barely depend on the angle of rotation for this wave function. The contrary occurs for (0, 1), where ξ_e raises specially for $\theta > 60°$, and the process cannot be selective using short pulses (the yield of selectivity being greater than 0.95 for defining ξ_s). In fact, increasing the peak amplitude one finds an asymptotic maximum yield, which depends on the angle of rotation, as shown in Figure 6. For $\theta = 90°$ this yield is zero. Obviously there is a symmetry rule forbidding this transition.[26]

The dependence of the asymptotic yield (and ξ_s) on θ can be partially explained in terms of the Franck−Condon factors that govern the dynamics. Since $V_2(r_1, r_2)$ is exactly equal to $V_1(r_1, r_2)$, despite being off-resonant, the initial state is only coupled to a single intermediate state, with the exact form as the initial one. Therefore, the adiabatic passage between the initial state in $V_1(r_1, r_2)$ and the target state in $V_3(r_1, r_2)$ will mainly depend on direct overlap between the initial and target states, which we show in Figure 7. The Franck−Condon factor between the (0, 0) wave function of V_1 and the (0, 0) wave function in V_3 barely depends on θ, which reflects the minor

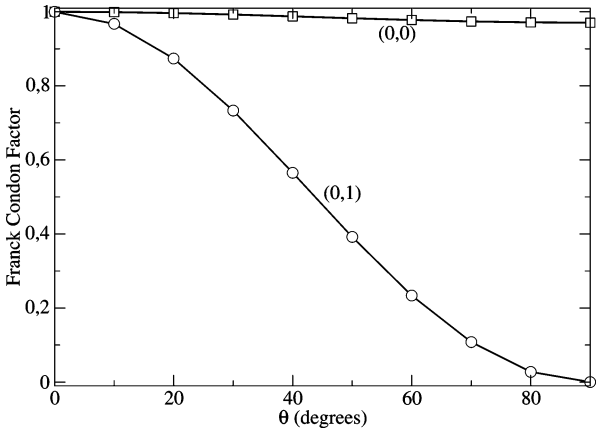

Figure 7. Franck-Condon factor between the (0, 0) states and the (0, 1) states in the initial and final potentials, as a function of the angle of rotation θ.

dependence of ξ_s on θ. However, the Franck−Condon factor between the (0, 1) states in V_1 and V_3 steadily decreases reaching zero for $\theta = 90°$: at this point (0, 1) in V_1 is exactly equal to (1, 0) in V_3 and therefore orthogonal to the target state. In fact, for both SPM and APM with pure rotation, the dynamics has intermediate features between StiRAP and APLIP: the selectivity depends mainly on a single intermediate state acting as a wave function bridge as in StiRAP; however, the pulse intensity and detuning allows several other pathways to promote the population to the excited potential, as in APLIP.

The existence of a nonzero Franck−Condon factor for θ different than 90° implies that the selective excitation should be possible, even if with stronger fields that compensate for the smallness of the coupling. In Figure 8 we analyze the breakdown of the selective adiabatic passage following the quasi-energies of the vibrational states of $U_0(r_1, r_2, t)$ as it evolves in time, for $\theta = 80°$ and the same pulse parameters. The eigenvalues of the LIP were obtained using the Fourier Grid Hamiltonian method.[27] $U_0(r_1, r_2, t)$ is mainly constructed as a linear combination of $V_1(r_1, r_2)$ and $V_3(r_1, r_2)$, the degree of the mixing being controlled by the pulse amplitudes. Therefore, $U_0(r_1, r_2, t)$ must twist as the normal coordinate axis change from those of the ground to those of the excited potential. This induces a small avoided crossing between the eigenvalues corresponding to the different vibrational dressed states with

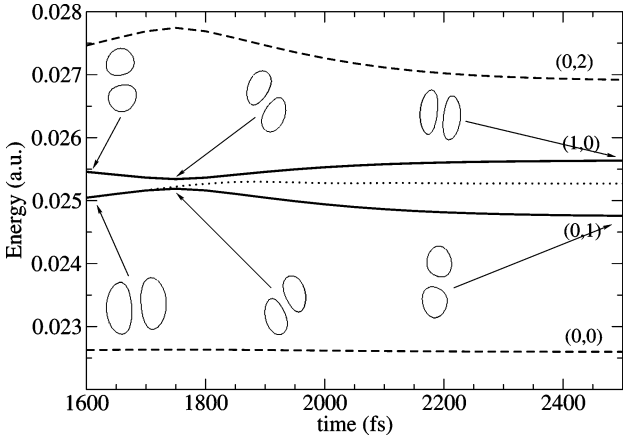

Figure 8. Dynamics of APLIP in the region of small avoided crossings. We show the frequency and shape of the vibrational states of the LIP as a function of time, for $\theta = 80°$. The (0, 1) and (1, 0) states almost cross as the normal axis of the LIP twist from the initial to the target state configurations.

the same sum of vibrational quanta. For instance, we observe in Figure 8 that during a small interval of time (at maximum peak amplitude of the lasers) there is a small avoided crossing between the eigenvalues corresponding to (0, 1) and (1, 0) of the LIP. Although the energy gap increases with the peak amplitude, finally one needs a minimum time to sweep adiabatically across the avoided crossing region. Therefore the APLIP scheme can only work using longer time pulses. Alternatively, the adiabatic thresholds imply weaker pulses, as Figure 6 shows.

A rough estimate of the minimum time and the adiabatic thresholds can be obtained assuming an StiRAP-type adiabatic passage. The effective nonresonant two-photon Rabi frequency is $\Omega_{\text{eff}} \sim \mu_{\text{if}}^2 \epsilon_0^2/2\Delta$,[23] where μ_{if} is the state-to-state transition dipole, that is, μ_{if}^2 is the Franck−Condon factor between the initial and the target state, shown in Figure 7. In order to have adiabatic passage to the target state, one needs $\Omega_{\text{eff}}\tau \geq 2\pi$ (to ensure around 95% of population). However, at the same time one must avoid the competing two-photon process that leads to the (1, 0) state. The Rabi frequency for this process ($\Omega_{\text{eff}}^{\perp}$) has the same form as the one before, with a different Franck−Condon factor, which is practically $1 - \mu_{\text{if}}^2$. The (1, 0) state is off resonance for the two-photon absorption, so that the yield of this process will become important only if $\Omega_{\text{eff}}^{\perp} \geq \Delta\omega$, where $\Delta\omega$ is the energy difference between the target state (0, 1) and (1, 0), that is, the shift from the resonance. In our model $\Delta\omega \sim 8{\cdot}10^{-4}$ au.

For $\theta = 70°$, $\mu_{\text{if}}^2 = 0.11$. When $\tau = 0.5$ ps, the adiabatic threshold will be reached with $\Omega_{\text{eff}} \sim 3{\cdot}10^{-4}$ au requiring $\epsilon_0 \sim 1.1{\cdot}10^{-2}$ au (comparable with what we obtain numerically). However, at this laser amplitude $\Omega_{\text{eff}}^{\perp} \sim 2.5{\cdot}10^{-3}$au $\gg \Delta\omega$, so that the adiabatic passage leads to (1, 0) essentially. Only with longer pulses ($\tau = 3$ ps) one obtains $\Omega_{\text{eff}} \sim 5{\cdot}10^{-5}$ au and $\Omega_{\text{eff}}^{\perp} \sim 4{\cdot}10^{-4}$ au allowing selective adiabatic passage with $\epsilon_0 \sim 4.3{\cdot}10^{-3}$ au. The same type of calculation can be used to show that for $\theta = 60°$, $\Omega_{\text{eff}}^{\perp}$ is of the order of $\Delta\omega$ already for shorter pulses ($\tau = 0.5$ ps), while for $\theta = 80°$, following our simple model, one would need 6 ps pulses in order to achieve selective adiabatic passage.

To summarize, we have observed that even without a true energy barrier, we need some extra energy coming from the laser in order to rotate the wave packet (or distort the LIP) and ensure the adiabatic passage. From the numerical results we observe that this adiabatic demand is practically the same for both APM and SPM models.

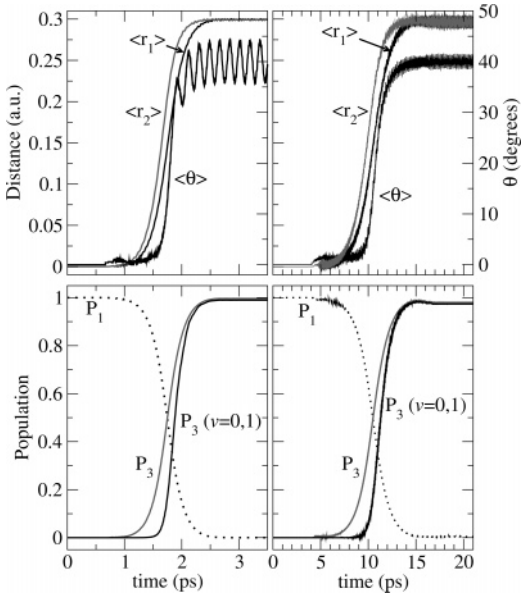

Figure 9. Dynamics of APLIP with translated [$d = (0.3, 0.3)$] and rotated ($\theta = 40°$) excited potentials using shorter (left) and longer (right) laser pulses. In both cases the initial state is (0, 1) and $\epsilon_0 = 0.087$ au. We show the average positions $\langle r_1(t)\rangle$ and $\langle r_2(t)\rangle$ (left scale) and angle $\langle\theta(t)\rangle$ (right scale) in the upper frames and the population histories in the lower frames.

5. Two-Dimensional Adiabatic Rotation and Displacement of the Wave Function

In this section we study the APLIP process when the target potential is both displaced and rotated with respect to the ground potential. In all the results of this section we fix $\vec{d} = (0.3, 0.3)$ and change the rotation angle θ using both SPM and APM set of parameters and pulses of different time durations. The dynamics requires the adiabatic translation and twisting of the wave packet as it adapts to the distorted LIP. In Figure 9 we show the population history and average observables of the wave packet in the adiabatic regime for $\theta = 40°$. Since $V_2(r_1, r_2)$ is also displaced with respect to $V_2(r_1, r_2)$ (by $\vec{d}/2$), several intermediate states can be used during the adiabatic transfer, and the dynamics clearly exhibits the APLIP signature of transient population on excited vibrational states both in the ground and target potentials.

The average observables provide interesting information regarding the dynamics. We define $\langle r_\alpha(t)\rangle = \langle\psi_0(\vec{r}, t)|r_\alpha|\psi_0(\vec{r}, t)\rangle$, where $\psi_0(\vec{r}, t)$ is the adiabatic wave packet in the U_0 LIP. The average angle of rotation of the wave function with respect to the initial state, $\langle\theta(t)\rangle$, is not a direct observable and can only be inferred with respect to a chosen axis of orientation. For the (0, 1) initial wave function the initial $\theta(0) = 0°$ corresponds to choosing r_2 as the "x" axis. Then the cosine square of the angle will be the projection of the wave packet onto the r_2 axis, which must be shifted to the average position of the wave packet, $(r_2 - \langle r_2\rangle)/(\vec{r} - \langle\vec{r}\rangle)$. Normalizing, we obtain for the angle

$$\cos^2\langle\theta(t)\rangle = \frac{\left|\left\langle \frac{r_2 - \langle r_2\rangle}{|\vec{r} - \langle\vec{r}\rangle|}\middle|\psi_0(\vec{r}, t)\right\rangle\right|^2}{\left|\left\langle \frac{r_1 - \langle r_1\rangle}{|\vec{r} - \langle\vec{r}\rangle|}\middle|\psi_0(\vec{r}, t)\right\rangle\right|^2 + \left|\left\langle \frac{r_2 - \langle r_2\rangle}{|\vec{r} - \langle\vec{r}\rangle|}\middle|\psi_0(\vec{r}, t)\right\rangle\right|^2} \quad (7)$$

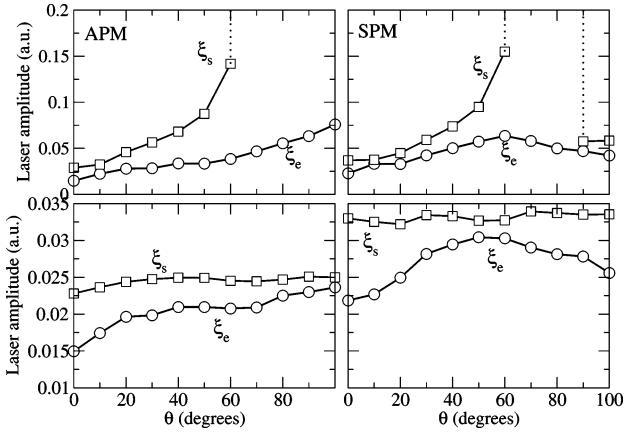

Figure 10. Adiabatic thresholds as a function of the rotating angle θ for translated excited potentials [$d = (0.3, 0.3)$] using the SPM (left) and APM (right) models and shorter pulses. The initial state is (0, 1).

In Figure 9, for the results of the APM, we show that $\langle r_2(t)\rangle$ shifts earlier than $\langle r_2(t)\rangle$. This is reasonable since in the APM the energy barrier is smaller along r_2. On the contrary, in the SPM we find $\langle r_1(t)\rangle = \langle r_2(t)\rangle$. More interestingly, we always observe that the change in $\langle\theta(t)\rangle$ starts later and occurs more rapidly than the shifts in position. Partially because of this, it is also more difficult to avoid some fluctuations in the angle (perfect adiabatic transfer) without using longer pulses.

In Figure 10 we show the electronic and selective thresholds of population transfer for both the APM and SPM model using shorter pulses. The selective transfer is not possible with $\theta > 60°$. However, as opposed to the case of rotation alone, the thresholds do not simply increase for larger θ. Additionally, the selective excitation at $\theta = 90°$ is not forbidden (even for short pulses we reach the selective threshold in the SPM), and the results are not symmetrical around this angle. The results for the SPM and APM differ more considerably than before, and we observe that the adiabatic demands are slightly larger when the source of rotation comes from the kinetic energy coupling, except for large θ.

A more detailed analysis of the behavior of the yield of the transfer as a function of the laser amplitude for large θ is shown in Figure 11. We consider the dynamics in the APM for shorter and longer pulses. Although the electronic transfer is perfectly adiabatic, the final population on the target state (0, 1) oscillates before reaching the selective adiabatic threshold. In fact, the final wave function is a superposition of (0, 1) and (1, 0). As in the case of rotation alone, this is due to a small avoided crossing for large θ. However, instead of reaching a plateau, the superposition changes with the amplitude. For intermediate values the avoided crossing can be made so small that all the population is selectively transferred to (1, 0), while for very large amplitude the transfer selects the original quantum state. Qualitatively the same type of behavior is also observed when using longer pulses.

6. Conclusions

Using two-dimensional harmonic oscillators as a molecular model, we have shown that the APLIP process is in principle feasible in polyatomic molecules. The adiabatic thresholds depend mainly on the characteristics of the energy barrier and therefore do not scale with the dimensionality of the system but only with the energy involved in the spatial distance (the bond elongations) that the wave function must cover to reach the target destination. Additionally, we have tested the effect of intramolecular energy transfer between the vibrational modes

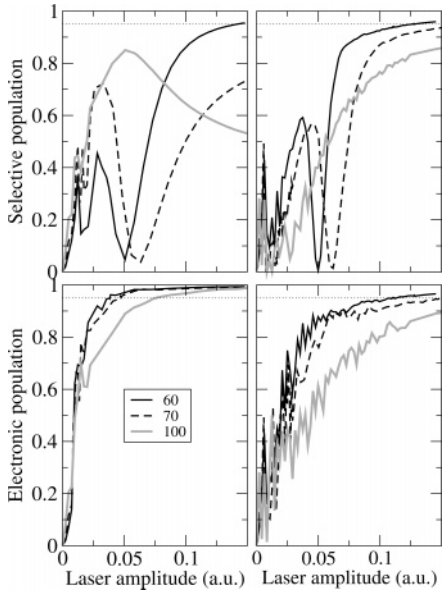

Figure 11. Final population in APLIP with translated and rotated excited potential, in the APM using shorter (left frames) and longer (right frames) pulses, for different rotation angles θ. The initial state is (0, 1).

in the form of Duschinsky couplings. Again, the transfer can be efficient and selective, except for rather unlikely molecular configurations. In principle, the adiabatic passage leads to a single eigenstate of the target potential in the adiabatic representation, which is obtained by diagonalizing the intramolecular coupling terms. This implies the rotation of the wave function, which can be selective when the initial state leads (without rotation) to a final superposition state or even to an orthogonal state.

In this paper we have used quite simplified models, but we believe that the models contain the majority of the essential features that can hinder the APLIP process. The shape of the potentials has been shown not to determine the outcome of the APLIP transfer. We consider only two-dimensional systems, but we have shown that the dimensionality is not a major concern, except for calculations. Obviously the role of intramolecular couplings may deter the selectivity of the transfer. We have shown how this may occur, in the frame of the Duschinsky effect, for two models: in one all the couplings enter into the kinetic energy and in the other the couplings occur in the potentials. In both cases the dynamics may proceed through regions of small avoided crossings, which tend to increase as the density of states becomes larger. Then, the state selectivity typically requires stronger and, more importantly, longer pulses, and the adiabatic demands increase, even when the bond elongation involved is rather small. These problems normally affect in a minor way the ground vibrational eigenfunction but become predominant when involving vibrationally excited wave functions coupled to more vibrational modes, i.e., higher dimensional systems. The same effects are expected for other forms of energy transfer among the modes, since the principles of APLIP imply an eigenstate specific transfer to the target adiabatic Born−Oppenheimer potential, regardless of the nature of the couplings.

In our models we have not included the effects of rotation and conical intersections. Since the transfer occurs in a single adiabatic potential, we believe that the strong pulses will induce adiabatic alignment.[28−30] The direction of the alignment will change in time adapting to the specific electronic mixture that configures the light-induced potential. Then, the adiabatic

rotational wave packet should not interfere with the vibrational adiabatic dynamics.[31]

On the other hand, conical intersections in the target potential can obviously drive part of the wave packet to uncontrolled parts of the Hamiltonian. The APLIP dynamics relies on isolating the ground and target potentials from other electronic states. In principle, with strong nonresonant pulses it is even possible to dynamically shift the position of the conical intersections, although it will be difficult to control at the same time the APLIP process.

Finally, although APLIP prepares a single eigenstate of the target adiabatic Born−Oppenheimer potential, it is not possible to guarantee the selectivity for strange molecular topologies, like double well structures, where the couplings are very weak.[19] In fact, the main experimental problems associated with APLIP are the ones observed already for simple diatomic molecules: the need to isolate the LIP from multiphoton or unwanted transitions yet using very strong laser pulses. Therefore, the search for physical systems, either diatomic or polyatomic, where these conditions can be met as best as possible, is under way.

Acknowledgment. Financial support from the Dirección General de Investigación Científica y Técnica under Project BQU2002-00173/ is gratefully acknowledged. J. G.-V. thanks the Spanish Ministry of Education and Science for his FPI Grant.

References and Notes

(1) Rabitz, H.; de Vivie-Riedle, R.; Motzkus, M.; Kompa, K. *Science* **2000**, *288*, 824.

(2) Rice, S. R.; Zhao, M. *Optimal control of molecular dynamics*; John Wiley & Sons: New York, 2000.

(3) Brumer, P.; Shapiro, M. *Principles of the Quantum Control of Moelecular Processes*; John Wiley & Sons: New York, 2003.

(4) Allen, L.; Eberly, J. H. *Optical Resonance and Two Level Atoms*; Dover: New York, 1975.

(5) Vitanov, N. V.; Halfmann, T.; Shore, B. W.; Bergmann, K. *Annu. Rev. Phys. Chem.* **2001**, *52*, 763.

(6) Oreg, J.; Hioe, F. T.; Eberly, J. H. *Phys. Rev. A* **1984**, *29*, 690.

(7) Gaubatz, U.; Rudecki, P.; Schiemann, S.; Bergmann, K. *J. Chem. Phys.* **1990**, *92*, 5363.

(8) Bergmann, K.; Theuer, H.; Shore, B. W. *Rev. Mod. Phys.* **1998**, *70*, 1003.

(9) Malinovsky, V. S.; Santamaria, J.; Sola, I. R. *J. Phys. Chem. A* **2003**, *107*, 8259.

(10) Garraway, B. M.; Suominen, K.-A. *Phys. Rev. Lett.* **1998**, *80*, 932.

(11) Chang, B. Y.; Rabitz, H.; Sola, I. R. *Phys. Rev. A.* **2003**, *68*, 031402.

(12) Sola, I. R.; Chang, B. Y.; Malinovsky, V. S.; Santamaria, J. In *Femtochemistry and Femtobiology*; Martin, M. M., Hynes, J. T., Eds.; Elsevier: 2004.

(13) Bandrauk, A. D.; Aubanel, E. E.; Gauthier, J.-M. In *Molecules in Laser Fields*; Bandrauk, A. D., Ed.; Dekker: New York, 1994.

(14) Aubanel, E. E.; Bandrauk, A. D.; *J. Phys. Chem.* **1993**, *97*, 12620.

(15) Sola, I. R.; Santamaría, J.; Malinovsky, V. S. *Phys. Rev. A* **2000**, *61*, 043413.

(16) Sola, I. R.; Chang, B. Y.; Santamaría, J.; Malinovsky, V. S.; Krause, J. L. *Phys. Rev. Lett.* **2000**, *85*, 4241.

(17) Rodriguez, M.; Suominen, K.-A.; Garraway, B. M. *Phys. Rev. A* **2000**, *62*, 053413.

(18) Chang, B. Y.; Sola, I. R.; Santamaría, J.; Malinovsky, V. S.; Krause, J. L. *J. Chem. Phys.* **2001**, *114*, 20.

(19) Malinovsky, V. S.; Krause, J. L. *Chem. Phys.* **2001**, *47*, 267.

(20) Although in this work we only consider the original APLIP scheme[10,15] with blue shifted lasers and counterintuitive sequences, APLIP can also work with intuitive pulse sequences shifted to the red of the intermediate potential.[16] Moreover, with some restrictions, all possible arrangements of time delays and detunings can also lead to the desired APLIP process.[18]

(21) Herzberg, G. *Molecular Spectra and Molecular Structure*; Van Nostrand: New York, 1945; Vol. III.

(22) Tannor, D. J.; Heller, E. J. *J. Chem. Phys.* **1982**, *77*, 202.

(23) Shore, B. W. *Theory of Coherent Atomic Excitation*; John Wiley & Sons: New York, 1990.

(24) Kosloff, R. *J. Phys. Chem.* **1988**, *92*, 2087.

(25) Wilson, E. B.; Decius, J. C.; Cross, P. C. *Molecular vibrations: The theory of Infrared and Raman Vibrational Spectra*; Dover: 1980.

(26) This symmetry rule is not observed if the intermediate potential is rotated at a different angle than those of the initial and target potentials.

(27) Marston, C. C.; Balint-Kurti, G. G. *J. Chem. Phys* **1989**, *91*, 3571.

(28) Friedrich, B.; Herschbach, D. *Phys. Rev. Lett.* **1995**, *74*, 4623.

(29) Friedrich, B.; Herschbach, D. *J. Phys. Chem.* **1995**, *99*, 15686.

(30) Friedrich, B.; Herschbach, D. *Chem. Phys. Lett.* **1996**, *262*, 41.

(31) Légaré, F.; Chelkowski, S.; Bandrauk, A. D. *Chem. Phys. Lett.* **2000**, *329*, 469.